

---

---

# Mechanical Analysis of Point Anchored Rock Bolt and Double Linings Support in Circular Hydraulic Tunnel

Y. J. Liu<sup>a,\*</sup>, B. S. Huang<sup>a</sup>, M. D. Yuan<sup>a</sup>, and E. H. Zhu<sup>a</sup>

<sup>a</sup>*Guangdong Research Institute of Water Resources and Hydropower, Guangzhou, 510610 China*

*\*e-mail: gdsylyj@163.com*

Received August 24, 2022; revised October 13, 2022; accepted October 15, 2022

**Abstract**—Rock bolt and lining are very common and effective support ways, and they are often used together in many projects because their bearing and reinforcement effects. However, the mechanism of the two support methods in the surrounding rock is not clear, especially the theoretical analysis. Therefore, a model is put forward to analyze the mechanical behavior of a deeply buried circular hydraulic tunnel jointly supported by double-linings and point anchored rock bolts, in which rock mass, double linings and bolts maintain elastic state and are in full contact with each other. And point anchored rock bolts are creatively replaced by pairs of concentrated forces of equal magnitude and opposite direction. By using the complex function method, the linear equations for solving the axial force of the bolts and the relevant analytical function coefficients can be established, based on the stress condition of the inner boundary of the secondary lining, continuity condition between the primary lining and the surrounding rock, and continuity condition between the primary lining and the secondary lining, as well as the compatibility condition of the displacement between the bolts and the surrounding rock. Then, using the analytical functions, the stress and displacement of any point in the double linings and surrounding rock can be calculated. Besides, the influence of inner hydrostatic pressure and exchange of Young's modulus of double linings are discussed, in which the support laws and mode of load transmission are analyzed. The results are in line with actual laws and can provide guiding suggestions for the design and construction of support works.

**Keywords:** circular hydraulic tunnel, point anchored rock bolt, double linings, combined support, axial force of bolt, stress and displacement solution

**DOI:** 10.3103/S0025654422601112

## 1. INTRODUCTION

In the 1950s, the New Austrian Tunneling Method (NATM) (Rabcewicz) was proposed and has been widely used in geotechnical engineering around the world, whose idea is to mobilize the strength and self-bearing capacity of surrounding rock as much as possible [1–7]. Therefore, shotcrete (lining) and bolts are widely recognized as effective support methods and are often used in support engineering at the same time, which can effectively restrict the deformation and improve the stress state of surrounding rock [8].

The lining (shotcrete) is a ring-shaped supporting structure close to the tunnel, which deforms harmoniously with the surrounding rock. It can not only limit the deformation of rock mass and provide support force for tunnel wall, but also close the surrounding rock and prevent its weathering. Through field test, model test, theoretical analysis and numerical simulation, scholars have been exploring the support principle of lining [2–5, 9–14]. These studies confirmed the role of lining, and considered various influencing factors, such as the roughness of contact surface, the development degree of rock joints, the spatial effect of excavation surface and the supporting time. Among them, the complex function method proposed by Muskhelishvili is a useful analytical method to analyze the interaction between rock mass and lining [11–16]. At present, the analytical solutions of stress and displacement for an arbitrarily shaped tunnel with lining in infinite domain can be obtained [13, 14]. Similar method will be used in this paper, and double linings are taken into consideration. As for bolting support, by placing rod-shaped reinforcement in the surrounding rock and grouting, the bolts and the rock mass are bonded together. The integrity and strength of the surrounding rock are enhanced by making full use of the characteristics of large stiffness and tension of the bolts, so as to maintain the stability of the excavated tunnel. Two types of rock bolts can be distinguished [17]: (1) point anchored rock bolts; and (2) fully grouted rock bolts. And there have been a lot of

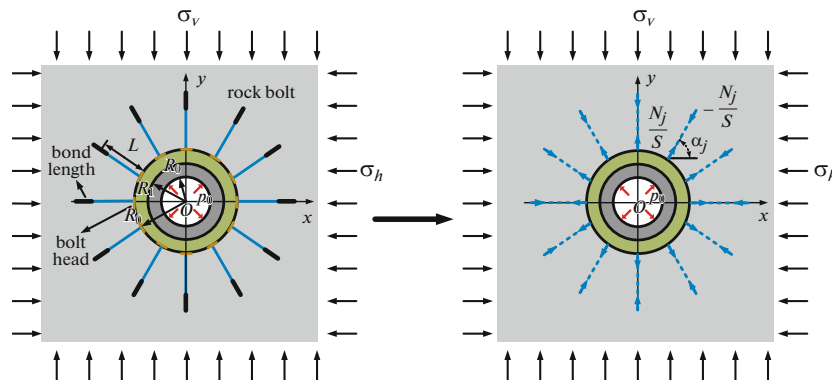


Fig. 1. The equivalent action of point anchored rock bolts.

researches on the anchoring principle of bolts [18–28]. Farmer [24] studied the shear stress distribution of anchorage interface and axial force of bolts by pull-out test. Freeman [25] proposed the neutral point theory through field observations. Bjurström [26] studied the effect of bolt on increasing the strength of jointed rock mass through shear test. Benmokrane et al. [27] proposed bond-slip model of rock bolt to establish the relationship between generated shear bond stress and relative displacement at the anchorage interface. Bernaud et al. [28] presented the numerical modelling of bolts with homogenization approach in a finite element procedure. In 2006, Bobet [29] first proposed an analytical method for analysis of point anchored rock bolts in circular tunnel in elastic ground. Similarly, in 2019, Lu [23] obtained the analytical method for analysis of the point anchored rock bolts in elliptical tunnel by using the complex function. Their common idea is to simplify the load acting on the surrounding rock by the point anchored rock bolt into a pair of concentrated forces with the equal magnitude and opposite direction, then solve the axial forces of bolts. This paper will also continue this idea to solve the interaction problem between rock mass and bolts.

NATM combines the advantages of bolt and lining and has been widely used. And researchers have been doing works on its mechanical mechanism and obtained many important conclusions by different ways. Chen et al. [30] presented the an equivalent constitutive model for jointed rock masses reinforced by bolt and lining and its implementation in a finite element program. They discussed the effect of the bolts and lining to the stiffness and shear resistance of the jointed rock mass. Holmgren and Ansell [31] studied the bolt anchored reinforced shotcrete lining subjected to impact loading. They pointed out that impact load caused the lining bond failure. And bolts can effectively absorb the impact load, but it needs a certain anchorage length. Sun and Zhang [32] established a circle model of composite support system consist of preliminary reinforcement, initial supports, secondary lining ring retainers and gave the internal force and deformation expression of arbitrary circle model by solving the problem of concentric composite rings. Ren et al. [33] conducted a three dimensional geomechanical model test based on similarity principle and numerical simulation. They found segmental lining played a major bearing role, while bolts played a role in strengthening rock mass. In addition, they discussed the influence of fault and plastic zone. Despite all this, the bolt-lining support design still mainly bases on engineering analogy method and engineering rock mass classification nowadays [34, 35], because the interaction mechanism between anchorage body and surrounding rock under complex geological conditions is not clear. The model established in this paper is based on the complex function method, which is a supplement to the principle research of bolt-linings combined support and can provide guidance for the early design of support.

As shown in Fig.1, the model adopted in this paper is to firstly install the point anchored rock bolts perpendicular to the tunnel wall, and then double linings support are applied. For the convenience of the analysis, it is assumed that the bolts and the double linings are installed at the same time. After the bolts are installed, they will deform along with the surrounding rock. Compared with the scale of surrounding rock, the influence of rock bolt diameter can be ignored. So the interaction between point anchored rock bolts and surrounding rock in deeply buried circular tunnel is simplified to a problem that multiple pairs of concentrated forces act on the vicinity of circular hole in an infinite domain. Besides, hydrostatic pressure  $p_0$  acts on the inner boundary of the secondary lining.

This paper assumes that the tunnel is deeply buried, rock mass, double linings and rock bolts are always in elastic state under the in-situ stress, and the strain along axis direction of tunnel is zero. That is to say, it is plane strain condition. The primary lining and surround rock is complete contact, which means the

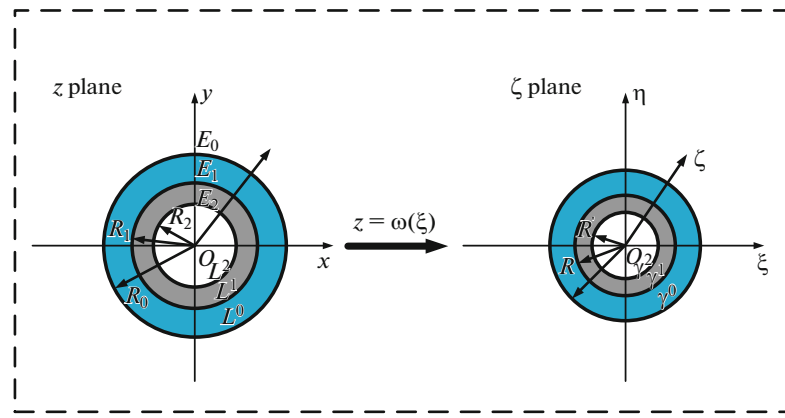


Fig. 2. Lined circular tunnel and ring-shaped region in the  $\zeta$  plane.

contact stress and the displacement at their interface is continuous. And the contact relationship between the primary lining and the secondary lining is the same. In addition, the action positions of the concentrated forces are assumed to be at the two effective ends of the bolts, that is, at the tunnel wall and the midpoint of the anchorage section. Despite some assumptions, the solution also has practical significance because the key variables, which influence the combined support system, can be readily identified and their relative importance can be quickly estimated.

## 2. FUNDAMENTAL PRINCIPLES AND EQUATIONS

### 2.1 Analytic Functions Considering Lining Installation Process

Firstly, we recur to the conformal transformation to map the double linings and the outer region of the tunnel into concentric circles and the outer region of a unit circle, respectively. See Fig. 2. And the mapping function is as follows

$$z = \omega(\zeta) = R_0\zeta, \tag{2.1}$$

where  $R_0, R_1, R_2$  is the radius of the circular tunnel, primary lining and secondary lining, respectively;  $L^2, L^1, L^0$  is the inner boundary of the secondary lining, contact interface of primary lining and secondary lining, contact interface of surrounding rock and primary lining, respectively.  $E_0, E_1, E_2$  is the Young's modulus of the rock mass, primary lining and secondary lining, respectively.  $\zeta = \rho e^{i\theta}$ ,  $i = \sqrt{-1}$ ;  $\rho$  is the radius in the  $\zeta$  plane and  $\rho = r/R_0$ , where  $r$  is the polar radius in the  $z$  plane;  $\theta$  is the polar angle in the  $\zeta$  plane, the same with the polar angle in the  $z$  plane. After mapping, the radius of the circular tunnel, primary lining and secondary lining is set to 1,  $R(R_1/R_0), R'(R_2/R_0)$ , respectively. And  $L^2, L^1, L^0$  corresponds to  $\gamma^2, \gamma^1, \gamma^0$ .

After the primary lining support is applied, the surrounding rock interacts with the primary lining. The two analytic functions corresponding to the surrounding rock mass under the action of primary lining can be expressed as:

$$\varphi_0(\zeta) = a_0 + \sum_{k=1}^{\infty} a_k \zeta^{-k}, \quad \psi_0(\zeta) = b_0 + \sum_{k=1}^{\infty} b_k \zeta^{-k}. \tag{2.2}$$

On the other hand, the two analytic functions corresponding to the primary lining can be expressed by as:

$$\varphi_1(\zeta) = d_0 + \sum_{k=1}^{\infty} e_k \zeta^{-k} + \sum_{k=1}^{\infty} f_k \zeta^k, \quad \psi_1(\zeta) = g_0 + \sum_{k=1}^{\infty} p_k \zeta^{-k} + \sum_{k=1}^{\infty} q_k \zeta^k. \tag{2.3}$$

And similarly, the two analytic functions corresponding to the secondary lining can be expressed by as:

$$\varphi_2(\zeta) = h_0 + \sum_{k=1}^{\infty} m_k \zeta^{-k} + \sum_{k=1}^{\infty} n_k \zeta^k, \quad \psi_2(\zeta) = r_0 + \sum_{k=1}^{\infty} s_k \zeta^{-k} + \sum_{k=1}^{\infty} t_k \zeta^k. \tag{2.4}$$

The above  $a_0, a_k, b_0, b_k, d_0, e_k, f_k, g_0, p_k, q_k, h_0, m_k, n_k, r_0, s_k, t_k$  are all real numbers to be determined by the boundary conditions given below. The series is taken as a finite term  $Ne$  in this paper, as long as the value of  $Ne$  is large enough, the result can be also accurate enough.

Using  $\varphi_0(\zeta)$  and  $\psi_0(\zeta)$ ,  $\varphi_1(\zeta)$  and  $\psi_1(\zeta)$ ,  $\varphi_2(\zeta)$  and  $\psi_2(\zeta)$ , the displacement at any point within the surrounding rock restricted by the primary lining and the displacements at any point within the double linings can be solved respectively as follows:

$$2G_0(u_0^p + iu_0^\theta) = \frac{\bar{\zeta} \overline{\omega'(\zeta)}}{\rho |\omega'(\zeta)|} \left[ \kappa_0 \varphi_0(\zeta) - \frac{\omega(\zeta)}{\omega'(\zeta)} \overline{\varphi_0'(\zeta)} - \overline{\psi_0(\zeta)} \right], \quad (2.5)$$

$$2G_1(u_1^p + iu_1^\theta) = \frac{\bar{\zeta} \overline{\omega'(\zeta)}}{\rho |\omega'(\zeta)|} \left[ \kappa_1 \varphi_1(\zeta) - \frac{\omega(\zeta)}{\omega'(\zeta)} \overline{\varphi_1'(\zeta)} - \overline{\psi_1(\zeta)} \right], \quad (2.6)$$

$$2G_2(u_2^p + iu_2^\theta) = \frac{\bar{\zeta} \overline{\omega'(\zeta)}}{\rho |\omega'(\zeta)|} \left[ \kappa_2 \varphi_2(\zeta) - \frac{\omega(\zeta)}{\omega'(\zeta)} \overline{\varphi_2'(\zeta)} - \overline{\psi_2(\zeta)} \right], \quad (2.7)$$

where  $u^p, u^\theta$  are the radial and tangential displacement components, respectively, in the  $z$  plane;  $K_0 = 3 - 4\mu_0, K_1 = 3 - 4\mu_1, K_2 = 3 - 4\mu_2$ ;  $(\mu_0, G_0, E_0), (\mu_1, G_1, E_1), (\mu_2, G_2, E_2)$  are Poisson's ratio, shear modulus and Young's modulus of the rock mass, primary lining and secondary lining, respectively. And  $G_0 = E_0/[2(1 + \mu_0)], G_1 = E_1/[2(1 + \mu_1)], G_2 = E_2/[2(1 + \mu_2)]$ .

## 2.2. Analytic Functions Considering Bolts Installation Process

The tunnel excavation brings about the deformation of surrounding rock, and the rock bolts installed within the rock mass will restrain the deformation. At the same time, the deformation of surrounding rock will exert loads on the bolts, so the axial forces are generated. As mentioned above, the effect of point anchored rock bolts on the surrounding rock can be regarded as pairs concentrated forces with the equal magnitude and opposite direction along the length of the bolts. The analytic functions corresponding to the surrounding rock under the action of  $j$ -th concentrated force can be expressed as follows [22]:

$$\begin{aligned} \varphi_{(j)}(\zeta) = & -\frac{X_j + iY_j}{2\pi(1 + \kappa_0)} \ln \left( 1 + \frac{R_0}{c_j} \zeta \right) - \frac{\kappa_0(X_j + iY_j)}{2\pi(1 + \kappa_0)} \ln \left( 1 + \frac{R_0}{c_j} \frac{1}{\zeta} \right) \\ & + \frac{X_j - iY_j}{2\pi(1 + \kappa_0)} \left( \frac{c_j \bar{c}_j - R_0^2}{c_j} \right) \frac{\zeta}{R_0 + \bar{c}_j \zeta}, \end{aligned} \quad (2.8)$$

$$\begin{aligned} \psi_{(j)}(\zeta) = & \frac{\kappa_0(X_j - iY_j)}{2\pi(1 + \kappa_0)} \ln \left( 1 + \frac{R_0}{c_j} \zeta \right) + \frac{X_j - iY_j}{2\pi(1 + \kappa_0)} \ln \left( 1 + \frac{R_0}{c_j} \frac{1}{\zeta} \right) \\ & - \frac{X_j + iY_j}{2\pi(1 + \kappa_0)} \frac{\bar{c}_j}{c_j + R_0 \zeta} + \frac{X_j + iY_j}{2\pi(1 + \kappa_0)} \frac{R_0}{c_j \zeta} - \frac{\kappa_0(X_j + iY_j)}{2\pi(1 + \kappa_0)} \frac{R_0}{\zeta^2 (R_0 + \bar{c}_j \zeta)} \\ & - \frac{X_j - iY_j}{2\pi(1 + \kappa_0)} \frac{c_j \bar{c}_j - R_0^2}{c_j} \frac{R_0}{\zeta (R_0 + \bar{c}_j \zeta)^2}, \end{aligned} \quad (2.9)$$

where  $X_j, Y_j$  are the component forces of  $j$ -th concentrated force acting on the surrounding rock on  $x$  and  $y$  axis respectively;  $c_j$  is radius vector from the position of the concentrated force to the center of circle tunnel. For the case that the concentrated force acts on the tunnel boundary, Eq. (2.8) and (2.9) are valid as well, namely  $|c_j| = R_0$ .

Based on the simplified bolts model, one of the concentrated forces acts outwards at the boundary of the tunnel, and the other one acts inwards at the midpoint of bond length (see Fig. 1). Let  $N_j$  denote the axial force of the  $j$ -th rock bolt. If the spacing of the rock bolts in the axial direction of the tunnel is  $S$ , then we have the following equations:

$$\begin{cases} X_j = N_j \cos \alpha_j / S; & Y_j = N_j \sin \alpha_j / S \\ X_{j+n} = -N_j \cos \alpha_j / S; & Y_{j+n} = -N_j \sin \alpha_j / S \end{cases} \quad (j = 1, 2, \dots, n), \quad (2.10)$$

$$\begin{cases} c_j = (-R_0 \cos \alpha_j) + i(-R_0 \sin \alpha_j) \\ c_{j+n} = [-(R_0 + L) \cos \alpha_j] + i[-(R_0 + L) \sin \alpha_j] \end{cases} \quad (j = 1, 2, \dots, n), \quad (2.11)$$

where  $\alpha_j$  is the  $j$ -th ( $j = 1, 2, \dots, n$ ) rock bolt installment angle, namely the angle between the outwards direction of the bolt and the  $x$  axis;  $n$  is the installation number of the point anchored rock bolts;  $L$  is the length between the effective ends of the bolts.

According to the superposition principle of elasticity, the analytic functions corresponding to the surrounding rock under the action of point anchored rock bolts can be obtained as follows:

$$\varphi_3(\zeta) = \sum_{j=1}^{2n} \varphi_{(j)}(\zeta), \quad \psi_3(\zeta) = \sum_{j=1}^{2n} \psi_{(j)}(\zeta). \quad (2.12)$$

Therefore, the displacements at any point within the surrounding rock under the action of the bolts can be solved as follows:

$$2G_0(u_3^p + iu_3^\theta) = \frac{\bar{\zeta}}{\rho} \frac{\overline{\omega'(\zeta)}}{|\omega'(\zeta)|} \left[ \kappa_0 \varphi_3(\zeta) - \frac{\omega(\zeta)}{\omega'(\zeta)} \overline{\varphi_3'(\zeta)} - \overline{\psi_3(\zeta)} \right], \quad (2.13)$$

where  $u_3^p$ ,  $u_3^\theta$  are the radial and tangential displacement components, respectively, in the  $z$  plane.

Combining Eqs. (2.8–2.13), the radial displacement  $u_3^p$  in any point  $(r, \theta)$  can be given as follows:

$$u_3^p(r, \theta) = \frac{1}{4\pi(1 + \kappa_0)G_0S} \sum_{j=1}^n \left[ N_j \sum_{l=1}^{10} h_l(\beta_j, \alpha_j, r, \theta) \right], \quad (2.14)$$

where:

$$\beta_j = |c_{j+n}|,$$

$$h_1(\beta_j, \alpha_j, r, \theta) = -\frac{R_0}{r} + \frac{R_0^2}{\beta_j r^2},$$

$$h_2(\beta_j, \alpha_j, r, \theta) = \frac{2R_0 r \sin^2(\theta - \alpha_j)}{R_0^2 - 2R_0 r \cos(\theta - \alpha_j) + r^2} - \frac{2\beta_j r \sin^2(\theta - \alpha_j)}{\beta_j^2 - 2\beta_j r \cos(\theta - \alpha_j) + r^2},$$

$$\begin{aligned} h_3(\beta_j, \alpha_j, r, \theta) &= \frac{\kappa_0 R_0 [R_0 \cos(\theta - \alpha_j) - r \cos(2\theta - 2\alpha_j)]}{R_0^2 - 2R_0 r \cos(\theta - \alpha_j) + r^2} \\ &\quad - \frac{\kappa_0 R_0^2 [R_0^2 \cos(\theta - \alpha_j) - \beta_j r \cos(2\theta - 2\alpha_j)]}{\beta_j^4 - 2\beta_j R_0^2 r \cos(\theta - \alpha_j) + \beta_j^2 r^2}, \end{aligned}$$

$$h_4(\beta_j, \alpha_j, r, \theta) = \frac{\kappa_0 r (\beta_j^2 - R_0^2) [-R_0^2 + \beta_j r \cos(\theta - \alpha_j)]}{\beta_j [R_0^4 - 2R_0^2 \beta_j r \cos(\theta - \alpha_j) + \beta_j^2 r^2]},$$

$$\begin{aligned} h_5(\beta_j, \alpha_j, r, \theta) &= -\frac{\kappa_0 R_0^3 [R_0 \cos(\theta - \alpha_j) - r \cos(2\theta - 2\alpha_j)]}{[R_0^2 - 2R_0 r \cos(\theta - \alpha_j) + r^2] r^2} \\ &\quad + \frac{\kappa_0 R_0^4 [R_0^2 \cos(\theta - \alpha_j) - \beta_j r \cos(2\theta - 2\alpha_j)]}{[R_0^4 - 2R_0^2 \beta_j r \cos(\theta - \alpha_j) + \beta_j^2 r^2] r^2}, \end{aligned}$$

$$h_6(\beta_j, \alpha_j, r, \theta) = -\frac{R_0^2 r (\beta_j^2 - R_0^2) [-R_0^4 + 2R_0^2 \beta_j r \cos(\theta - \alpha_j) - \beta_j^2 r^2 \cos(2\theta - 2\alpha_j)]}{\beta_j [R_0^4 - 2R_0^2 \beta_j r \cos(\theta - \alpha_j) + \beta_j^2 r^2]},$$

$$h_7(\beta_j, \alpha_j, r, \theta) = \frac{R_0^4 (\beta_j^2 - R_0^2) [-R_0^4 + 2R_0^2 \beta_j r \cos(\theta - \alpha_j) - \beta_j^2 r^2 \cos(2\theta - 2\alpha_j)]}{\beta_j r [R_0^4 - 2R_0^2 \beta_j r \cos(\theta - \alpha_j) + \beta_j^2 r^2]},$$

$$h_8(\beta_j, \alpha_j, r, \theta) = (\kappa_0^2 - 1) \sin(\theta - \alpha_j) \left\{ \tan^{-1} \left[ \frac{R_0 \sin(\theta - \alpha_j)}{-R_0 \cos(\theta - \alpha_j) + r} \right] - \tan^{-1} \left[ \frac{R_0^2 \sin(\theta - \alpha_j)}{-R_0^2 \cos(\theta - \alpha_j) + \beta_j r} \right] \right\},$$

$$h_9(\beta_j, \alpha_j, r, \theta) = \kappa_0 \cos(\theta - \alpha_j) \ln \left[ \frac{\beta_j^2 (R_0^2 - 2R_0 r \cos(\theta - \alpha_j) + r^2)}{R_0^2 (\beta_j^2 - 2\beta_j r \cos(\theta - \alpha_j) + r^2)} \right],$$

$$h_{10}(\beta_j, \alpha_j, r, \theta) = \frac{1}{2} (1 + \kappa_0^2) \cos(\theta - \alpha_j) \ln \left[ \frac{\beta_j^2 (R_0^2 - 2R_0 r \cos(\theta - \alpha_j) + r^2)}{R_0^4 - 2R_0^2 \beta_j r \cos(\theta - \alpha_j) + \beta_j^2 r^2} \right].$$

### 2.3. Analytic Functions Considering the Excavation of the Tunnel

The displacement  $u_4^p$  and  $u_4^\theta$  at any point in the surrounding rock mass due to circular tunnel excavation can be obtained by two analytic functions [15]:

$$\varphi_4(\zeta) = -\frac{\sigma_v - \sigma_h}{2\zeta} R_0, \quad (2.15)$$

$$\psi_4(\zeta) = -\frac{R_1}{2} \left( \frac{\sigma_v + \sigma_h}{\zeta} + \frac{\sigma_v - \sigma_h}{\zeta^3} \right), \quad (2.16)$$

$$u_4^p + iu_4^\theta = \frac{1}{2G_0 \rho} \frac{\overline{\omega'(\zeta)}}{|\omega'(\zeta)|} \left[ \kappa_0 \varphi_4(\zeta) - \frac{\omega(\zeta)}{\omega'(\zeta)} \overline{\varphi_4'(\zeta)} - \overline{\psi_4(\zeta)} \right], \quad (2.17)$$

where  $\sigma_v$  and  $\sigma_h$  are vertical and horizontal in-situ stress, respectively. The displacement shown in Eq. (2.17) is the total displacement in the surrounding rock when the tunnel is unsupported. If the tunnel displacement is supported after  $\eta$  ( $0 \leq \eta \leq 1$ ) times of the total displacement, the displacement of the surrounding rock before the support is  $\eta(u_4^p + iu_4^\theta)$ .  $\eta$  is the displacement release coefficient [12–14], which is determined by the distance between the working face and the lined section.

### 2.4. Equations of Solving $\varphi_0(\zeta)$ , $\psi_0(\zeta)$ , $\varphi_1(\zeta)$ , $\psi_1(\zeta)$ , $\varphi_2(\zeta)$ , $\psi_2(\zeta)$ and $N_j$

#### 2.4.1. Stress Condition of Inner Boundary of the Secondary Lining

Suppose that a uniform hydrostatic pressure  $p_0$  acts on the inner boundary of the secondary lining  $L^2$ , the stress boundary conditions along  $\gamma^2$  in the  $\zeta$  plane can be expressed as:

$$\varphi_2(R' \sigma) + \frac{\omega(R' \sigma)}{\omega'(R' / \sigma)} \overline{\varphi_2'(R' / \sigma)} + \overline{\psi_2(R' / \sigma)} = p_0 \omega(R' \sigma). \quad (2.18)$$

Substituting Eq. (2.4) into Eq. (2.18) leads to:

$$\begin{aligned} h_0 + \sum_{k=1}^{Ne} m_k R'^{-k} \sigma^{-k} + \sum_{k=1}^{Ne} n_k R'^k \sigma^k + \sum_{k=1}^{Ne} (-k) m_k R'^{-k} \sigma^{k+2} + \sum_{k=1}^{Ne} k n_k R'^k \sigma^{-k+2} \\ + r_0 + \sum_{k=1}^{Ne} s_k R'^{-k} \sigma^k + \sum_{k=1}^{Ne} t_k R'^k \sigma^{-k} = p_0 R_2. \end{aligned} \quad (2.19)$$

By comparing the coefficients of  $\sigma^{-Ne} \rightarrow \sigma^{Ne}$  in Eq. (2.19), the relationship of the coefficients can be obtained as follows:

$$\begin{cases} h_0 + 2n_2R^2 + r_0 = 0, \\ 2n_1R' + s_1R'^{-1} = p_0R_2, \\ n_2R'^2 + s_2R'^{-2} = 0, \\ -(k-2)m_{k-2}R'^{-(k-2)} + n_kR'^k + s_kR'^{-k} = 0; \quad 3 \leq k \leq Ne, \\ m_kR'^{-k} + (k+2)n_{k+2}R'^{k+2} + t_kR'^k = 0; \quad 1 \leq k \leq Ne-2, \\ m_{Ne-1}R'^{-(Ne-1)} + t_{Ne-1}R'^{Ne-1} = 0, \\ m_{Ne}R'^{-Ne} + t_{Ne}R'^{Ne} = 0. \end{cases} \quad (2.20)$$

#### 2.4.2. Contact Stress Continuity Conditions at the Interface Between the Primary Lining and the Surrounding Rock

Since the analytic function corresponding to the interaction between the surrounding rock and the lining are  $\varphi_0(\zeta)$  and  $\psi_0(\zeta)$ , the stress continuity conditions along the interface  $L^0$ , corresponding to  $\gamma^0$  in the  $\zeta$  plane, can be expressed as:

$$\varphi_0(\sigma) + \frac{\omega(\sigma)}{\omega'(\sigma)} \overline{\varphi_0'(\sigma)} + \overline{\psi_0(\sigma)} = \varphi_1(\sigma) + \frac{\omega(\sigma)}{\omega'(\sigma)} \overline{\varphi_1'(\sigma)} + \overline{\psi_1(\sigma)}. \quad (2.21)$$

Substituting Eq. (2.2) and Eq. (2.3) into Eq. (2.21) leads to:

$$\begin{cases} a_0 + b_0 = d_0 + 2f_2 + g_0, \\ b_1 = 2f_2 + p_1, \\ b_2 = f_2 + p_2, \\ -(k-2)a_{k-2} + b_k = f_k - (k-2)e_{i-2} + p_i; \quad 3 \leq k \leq Ne, \\ a_k = e_k + (k+2)f_{k+2} + q_k; \quad 1 \leq k \leq Ne-2, \\ a_{Ne-1} = e_{Ne-1} + q_{Ne-1}, \\ a_{Ne} = e_{Ne} + q_{Ne}. \end{cases} \quad (2.22)$$

#### 2.4.3. Displacement Compatibility Conditions at the Interface Between the Primary Lining and the Surrounding Rock

After the linings and rock bolts are applied, the surrounding rock and the primary lining still keep full contact with each other along the contact surface  $L^0$ , we can get the following equation by displacement compatibility condition:

$$(1 - \eta)(u_4^p + iu_4^\theta) - (u_0^p + iu_0^\theta) - (u_3^p + iu_3^\theta) = (u_1^p + iu_1^\theta). \quad (2.23)$$

Substituting Eqs. (2.5), (2.6), (2.13) and (2.17) into Eq. (2.23), through sorting we have:

$$\begin{aligned} & \sum_{j=1}^n \frac{N_j}{2G_0S} [\kappa_0 m_j - (\cos \theta + i \sin \theta) t_j - w_j] + \frac{1}{2G_0} \left\{ \kappa_0 a_0 + \sum_{k=1}^{Ne} [\kappa_0 (\cos k\theta - i \sin k\theta) \right. \\ & \quad \left. + k(\cos(k+2)\theta + i \sin(k+2)\theta)] a_k - b_0 - \sum_{k=1}^{Ne} b_k (\cos k\theta + i \sin k\theta) \right\} \\ & - \frac{1}{2G_1} \left\{ \kappa_1 d_0 + \sum_{k=1}^{Ne} [\kappa_1 (\cos k\theta - i \sin k\theta) + k(\cos(k+2)\theta + i \sin(k+2)\theta)] e_k \right. \\ & \quad \left. + \sum_{k=1}^{Ne} [\kappa_1 (\cos k\theta + i \sin k\theta) - k(\cos(2-k)\theta + i \sin(2-k)\theta)] f_k - g_0 \right\} \end{aligned} \quad (2.24)$$

$$\begin{aligned}
& -\sum_{k=1}^{Ne} (\cos k\theta + i \sin k\theta) p_k - \sum_{k=1}^{Ne} (\cos k\theta - i \sin k\theta) q_k \\
& = \frac{(1-\eta)R_0}{4G_0} [\kappa_0(\sigma_v - \sigma_h)(\cos \theta - i \sin \theta) - (\sigma_v + \sigma_h)(\cos \theta + i \sin \theta)],
\end{aligned}$$

where

$$\begin{aligned}
m_j = & \left[ \begin{aligned} & -\frac{\cos \alpha_j + i \sin \alpha_j}{2\pi(1 + \kappa_0)} \ln \left( 1 + \frac{R_0}{c_j \sigma} \right) - \frac{\kappa_0(\cos \alpha_j + i \sin \alpha_j)}{2\pi(1 + \kappa_0)} \ln \left( 1 + \frac{R_0}{c_j} \frac{1}{\sigma} \right) \\ & + \frac{\cos \alpha_j - i \sin \alpha_j}{2\pi(1 + \kappa_0)} \frac{c_j \bar{c}_j - R_0^2}{c_j} \frac{\sigma}{R_0 + c_j \sigma} \end{aligned} \right] \\
- & \left[ \begin{aligned} & -\frac{\cos \alpha_j + i \sin \alpha_j}{2\pi(1 + \kappa_0)} \ln \left( 1 + \frac{R_0}{c_{j+n} \sigma} \right) - \frac{\kappa_0(\cos \alpha_j + i \sin \alpha_j)}{2\pi(1 + \kappa_1)} \ln \left( 1 + \frac{R_0}{c_{j+n}} \frac{1}{\sigma} \right) \\ & + \frac{\cos \alpha_j - i \sin \alpha_j}{2\pi(1 + \kappa_0)} \frac{c_{j+n} \bar{c}_{j+n} - R_0^2}{c_{j+n}} \frac{\sigma}{R_0 + c_{j+n} \sigma} \end{aligned} \right], \quad (2.25)
\end{aligned}$$

$$\begin{aligned}
t_j = & \left[ \begin{aligned} & -\frac{\cos \alpha_j - i \sin \alpha_j}{2\pi(1 + \kappa_0)} \frac{R_0 \sigma}{R_0 + \bar{c}_j \sigma} + \frac{\kappa_0(\cos \alpha_j - i \sin \alpha_j)}{2\pi(1 + \kappa_0)} \frac{R_0 \sigma^2}{R_0 \sigma + c_j} \\ & + \frac{\cos \alpha_j + i \sin \alpha_j}{2\pi(1 + \kappa_0)} \frac{c_j \bar{c}_j - R_0^2}{c_j} \frac{R_0 \sigma^2}{(R_0 \sigma + c_j)^2} \end{aligned} \right] \\
- & \left[ \begin{aligned} & -\frac{\cos \alpha_j - i \sin \alpha_j}{2\pi(1 + \kappa_0)} \frac{R_0 \sigma}{R_0 + c_{j+n} \sigma} + \frac{\kappa_0(\cos \alpha_j - i \sin \alpha_j)}{2\pi(1 + \kappa_0)} \frac{R_0 \sigma^2}{R_0 \sigma + c_{j+n}} \\ & + \frac{\cos \alpha_j + i \sin \alpha_j}{2\pi(1 + \kappa_0)} \frac{c_{j+n} \bar{c}_{j+n} - R_0^2}{c_{j+n}} \frac{R_0 \sigma^2}{(R_0 \sigma + c_{j+n})^2} \end{aligned} \right], \quad (2.26)
\end{aligned}$$

$$\begin{aligned}
w_j = & \left[ \begin{aligned} & \frac{\kappa_0(\cos \alpha_j + i \sin \alpha_j)}{2\pi(1 + \kappa_0)} \ln \left( 1 + \frac{R_0}{c_j \sigma} \right) + \frac{\cos \alpha_j + i \sin \alpha_j}{2\pi(1 + \kappa_0)} \ln \left( 1 + \frac{R_0 \sigma}{c_j} \right) \\ & - \frac{\cos \alpha_j - i \sin \alpha_j}{2\pi(1 + \kappa_0)} \frac{c_j \sigma}{c_j \sigma + R_0} + \frac{\cos \alpha_j - i \sin \alpha_j}{2\pi(1 + \kappa_0)} \frac{R_0 \sigma}{c_j} \\ & - \frac{\kappa_0(\cos \alpha_j - i \sin \alpha_j)}{2\pi(1 + \kappa_0)} \frac{R_0 \sigma^3}{R_0 \sigma + c_j} - \frac{\cos \alpha_j + i \sin \alpha_j}{2\pi(1 + \kappa_0)} \frac{c_j \bar{c}_j - R_0^2}{c_j} \frac{R_0 \sigma^3}{(R_0 \sigma + c_j)^2} \end{aligned} \right] \\
- & \left[ \begin{aligned} & \frac{\kappa_0(\cos \alpha_j + i \sin \alpha_j)}{2\pi(1 + \kappa_0)} \ln \left( 1 + \frac{R_0}{c_{j+n} \sigma} \right) + \frac{\cos \alpha_j + i \sin \alpha_j}{2\pi(1 + \kappa_0)} \ln \left( 1 + \frac{R_0 \sigma}{c_{j+n}} \right) \\ & - \frac{\cos \alpha_j - i \sin \alpha_j}{2\pi(1 + \kappa_0)} \frac{c_{j+n} \sigma}{c_{j+n} \sigma + R_0} + \frac{\cos \alpha_j - i \sin \alpha_j}{2\pi(1 + \kappa_0)} \frac{R_0 \sigma}{c_{j+n}} \\ & - \frac{\kappa_0(\cos \alpha_j - i \sin \alpha_j)}{2\pi(1 + \kappa_0)} \frac{R_0 \sigma^3}{R_0 \sigma + c_{j+n}} - \frac{\cos \alpha_j + i \sin \alpha_j}{2\pi(1 + \kappa_0)} \frac{c_{j+n} \bar{c}_{j+n} - R_0^2}{c_{j+n}} \frac{R_0 \sigma^3}{(R_0 \sigma + c_{j+n})^2} \end{aligned} \right]. \quad (2.27)
\end{aligned}$$

Besides, the effect of the lining on the surrounding rock decreases as  $\zeta$  increases, that is, as  $\zeta \rightarrow \infty$ , corresponding to the infinity in the  $z$  plane, we have  $u_0^p \rightarrow 0$  and  $u_0^\theta \rightarrow 0$ . According to Eq. (2.5), the following equation can be obtained:

$$\lim_{\zeta \rightarrow \infty} [2G_0(u_0^p + iu_0^\theta)] = \lim_{\zeta \rightarrow \infty} \left\{ \frac{\bar{\zeta} \overline{\omega'(\zeta)}}{\rho |\omega'(\zeta)|} \left[ \kappa_0 \Phi_0(\zeta) - \frac{\alpha(\zeta)}{\omega'(\zeta)} \overline{\Phi_0'(\zeta)} - \overline{\Psi_0(\zeta)} \right] \right\} = 0. \quad (2.28)$$



Since  $\lim_{\zeta \rightarrow \infty} [\varphi_0(\zeta)] = a_0$ ,  $\lim_{\zeta \rightarrow \infty} \left[ \frac{\omega(\zeta)}{\omega'(\zeta)} \overline{\varphi_0'(\zeta)} \right] = 0$  and  $\lim_{\zeta \rightarrow \infty} [\psi_0(\zeta)] = d_0$ , according to Eq. (2.28), we have:

$$a_0 = d_0/\kappa_0. \quad (2.29)$$

#### 2.4.4. Displacement Compatibility Condition Between the Bolts and the Surrounding Rock

Due to the excavation of the tunnel, point anchored rock bolts interact with the surrounding rock. Before the failure of bolts, the points of connection (bolt head and midpoint of the anchorage section) between the surrounding rock and the adjacent bolts will always be bonded and deform together. Based on the displacement compatibility condition, we have:

$$(1 - \eta)\Delta u_4^p - \Delta u_0^p - \Delta u_3^p = \Delta u(\delta); \quad (\delta = 1, 2, \dots, n), \quad (2.30)$$

where  $\Delta u(\delta)$  is the elongation of the  $\delta$ -th rock bolt, which can be calculated as follows:

$$\Delta u(\delta) = \frac{4N_\delta L}{E_3 \pi d^2}; \quad (\delta = 1, 2, \dots, n), \quad (2.31)$$

where  $E_3$ ,  $d$  represent the Young's modulus and the diameter of the rock bolt, respectively.

Combine Eqs. (2.2), (2.5), (2.14–2.17) and (2.30–2.31), the displacement compatibility condition between  $\delta$ -th rock bolt and the rock mass can be obtained:

$$\begin{aligned} & \frac{1}{4\pi(1 + \kappa_0)G_0 S} \sum_{j=1}^n \left\{ N_j \sum_{i=1}^{10} [h_i(\beta_j, \alpha_j, R_0, \alpha_\delta) - h_i(\beta_j, \alpha_j, R_0 + L, \alpha_\delta)] \right\} \\ & + \frac{\cos \alpha_\delta - \sin \alpha_\delta}{2G_0} \left\{ \sum_{k=1}^{Ne} a_k [(1 + L/R_0)^{-k} (\cos k\alpha_\delta - i \sin k\alpha_\delta) \right. \\ & \quad \left. + k(1 + L/R_0)^{-k} (\cos(k+2)\alpha_\delta + i \sin(k+2)\alpha_\delta)] \right. \\ & \quad \left. - \sum_{k=1}^{Ne} b_k [(1 + L/R_0)^{-k} (\cos k\alpha_\delta - i \sin k\alpha_\delta)] \right\} \\ & - \frac{\cos \alpha_j - \sin \alpha_j}{2G_0} \left\{ \sum_{k=1}^{Ne} a_k [\cos k\alpha_\delta - i \sin k\alpha_\delta + k(\cos(k+2)\alpha_\delta \right. \\ & \quad \left. + i \sin(k+2)\alpha_\delta)] - \sum_{k=1}^{Ne} b_k (\cos k\alpha_\delta - i \sin k\alpha_\delta) \right\} - \frac{4N_\delta L}{E_3 \pi d^2} \\ & = \frac{(1 - \eta)}{2G_0} \left[ -\frac{1 + \kappa_0}{2} \frac{R_0(\sigma_v - \sigma_h)}{(1 + L/R_0)} \cos 2\alpha_\delta + \frac{R_0(\sigma_v - \sigma_h)}{2(1 + L/R_0)^3} \cos 2\alpha_\delta + \frac{R_0(\sigma_v + \sigma_h)}{2(1 + L/R_0)} \right] \\ & - \frac{(1 - \eta)}{2G_0} \left[ -\frac{1 + \kappa_0}{2} R_0(\sigma_v - \sigma_h) \cos 2\alpha_\delta + \frac{R_0(\sigma_v - \sigma_h)}{2} \cos 2\alpha_\delta + \frac{R_0(\sigma_v + \sigma_h)}{2} \right]. \end{aligned} \quad (2.32)$$

#### 2.4.5. Contact Condition Between the Primary Lining and the Secondary Lining

Since the primary lining and the secondary lining maintain complete contact at the interface, the following displacement coordination equation is satisfied:

$$\begin{aligned} & \frac{1}{2G_1 \rho} \frac{\bar{\zeta} \overline{\omega'(\zeta)}}{|\omega'(\zeta)|} \left[ \kappa_1 \varphi_1(\zeta) - \frac{\omega(\zeta)}{\omega'(\zeta)} \overline{\varphi_1'(\zeta)} - \overline{\psi_1(\zeta)} \right] \\ & = \frac{1}{2G_2 \rho} \frac{\bar{\zeta} \overline{\omega'(\zeta)}}{|\omega'(\zeta)|} \left[ \kappa_2 \varphi_2(\zeta) - \frac{\omega(\zeta)}{\omega'(\zeta)} \overline{\varphi_2'(\zeta)} - \overline{\psi_2(\zeta)} \right], \quad \zeta = Re^{i\theta}. \end{aligned} \quad (2.33)$$

Substituting Eqs. (2.3), (2.4) into Eq. (2.33), through sorting we have:

$$\left\{ \begin{array}{l}
\frac{1}{2G_1}[\kappa_1 d_0 + g_0 + 2f_2 R^2] - \frac{1}{2G_2}[\kappa_2 h_0 + r_0 + 2n_2 R^2] = 0, \\
\frac{1}{2G_1}[(\kappa_1 + 1)Rf_1 + R^{-1}p_1] - \frac{1}{2G_2}[(\kappa_2 + 1)Rn_1 + R^{-1}s_1] = 0, \\
\frac{1}{2G_1}(\kappa_1 R^2 f_2 + R^{-2}p_2) - \frac{1}{2G_2}[\kappa_2 R^2 n_2 + R^{-2}s_2] = 0, \\
\left\langle \frac{1}{2G_1}[\kappa_1 R^i f_i + (2-i)R^{2-i}e_{i-2} + R^{-i}p_i] \right. \\
\left. - \frac{1}{2G_2}[\kappa_2 R^i n_i + (2-i)R^{2-i}m_{i-2} + R^{-i}s_i] = 0 \right\rangle; \quad 3 \leq k \leq Ne, \\
\left\langle \frac{1}{2G_1}[\kappa_1 R^{-i}e_i + (2+i)R^{2+i}f_{i+2} + R^i q_i] \right. \\
\left. - \frac{1}{2G_2}[\kappa_2 R^{-i}m_i + (2+i)R^{2+i}n_{i+2} + R^i t_i] = 0 \right\rangle; \quad 1 \leq k \leq Ne - 2, \\
\frac{1}{2G_1}[\kappa_1 R^{1-Ne}e_{Ne-1} + R^{Ne-1}q_{Ne-1}] - \frac{1}{2G_2}[\kappa_2 R^{1-Ne}m_{Ne-1} + R^{Ne-1}t_{Ne-1}] = 0, \\
\frac{1}{2G_1}[\kappa_1 R^{-Ne}e_{Ne} + R^{Ne}q_{Ne}] - \frac{1}{2G_2}[\kappa_2 R^{-Ne}m_{Ne} + R^{Ne}t_{Ne}] = 0.
\end{array} \right. \quad (2.34)$$

For the same reason, the interface between the primary lining and the secondary lining meets the stress continuity condition:

$$\varphi_1(\zeta) + \frac{\omega(\zeta)}{\omega'(\zeta)} \overline{\varphi_1'(\zeta)} + \overline{\psi_1(\zeta)} = \varphi_2(\zeta) + \frac{\omega(\zeta)}{\omega'(\zeta)} \overline{\varphi_2'(\zeta)} + \overline{\psi_2(\zeta)}, \quad \zeta = Re^{i\theta}. \quad (2.35)$$

Substituting Eqs. (2.3), (2.4) into Eq. (2.35), through sorting we have:

$$\left\{ \begin{array}{l}
d_0 + g_0 + 2f_2 R^2 - h_0 - r_0 - 2n_2 R^2 = 0, \\
2Rf_1 + R^{-1}p_1 - 2Rn_1 - R^{-1}s_1 = 0, \\
R^2 f_2 + R^{-2}p_2 - R^2 n_2 - R^{-2}s_2 = 0, \\
R^i f_i + (2-i)R^{2-i}e_{i-2} + R^{-i}p_i - \kappa_2 R^i n_i - (2-i)R^{2-i}m_{i-2} - R^{-i}s_i = 0; \quad 3 \leq k \leq Ne, \\
R^{-i}e_i + (2+i)R^{2+i}f_{i+2} + R^i q_i - \kappa_2 R^{-i}m_i - (2+i)R^{2+i}n_{i+2} - R^i t_i = 0; \quad 1 \leq k \leq Ne - 2, \\
R^{1-Ne}e_{Ne-1} + R^{Ne-1}q_{Ne-1} - R^{1-Ne}m_{Ne-1} - R^{Ne-1}t_{Ne-1} = 0, \\
R^{-Ne}e_{Ne} + R^{Ne}q_{Ne} - R^{-Ne}m_{Ne} - R^{Ne}t_{Ne} = 0.
\end{array} \right. \quad (2.36)$$

To solve  $\varphi_0(\zeta)$  and  $\psi_0(\zeta)$ ,  $\varphi_1(\zeta)$  and  $\psi_1(\zeta)$ ,  $\varphi_2(\zeta)$  and  $\psi_2(\zeta)$ , and  $N_j$  ( $j = 1, 2, \dots, n$ ),  $10Ne + 6 + n$  unknown numbers need to be solved, that is:  $a_0, a_k, b_0, b_k, d_0, e_k, f_k, g_0, p_k, q_k, h_0, m_k, n_k, r_0, s_k, t_k$  ( $k = 1, 2, \dots, Ne$ ), as well as  $N_j$  ( $j = 1, 2, \dots, n$ ). Accordingly,  $10Ne + 6 + n$  linear equations can be established to solve these unknown numbers. That is:  $2Ne + 1$  linear equations about stress condition of inner boundary of the secondary lining in Eq. (2.20);  $2Ne + 1$  linear equations about contact stress condition at the interface between the primary lining and the surrounding rock in Eq. (2.22);  $2Ne + 1$  linear equations about displacement compatibility condition of the interface between the primary lining and the surrounding rock in Eq. (2.24) {let  $\theta = 2k\pi/(2Ne + 1)$ , ( $k = 1, 2, \dots, 2Ne + 1$ ) respectively, note that: avoid being too close to the anchoring head}; 1 linear equation about the effect of the primary lining on the surrounding rock at infinity in Eq. (2.29);  $n$  linear equations about the displacement compatibility condition between the bolts and the surrounding rock in Eq. (2.32) (Let  $\delta$  be equal to 1, 2, ...,  $n$ , respectively);  $2Ne + 1$  linear equations about displacement compatibility condition of the interface between the primary lining and the secondary lining in Eq. (2.34); and  $2Ne + 1$  linear equations about contact stress condition of the interface between the primary lining and the secondary lining in Eq. (2.36).

### 2.5. Solutions for the Stresses and Displacements in the Linings and Surrounding Rock

Since the analytic functions  $\varphi_0(\zeta)$  and  $\psi_0(\zeta)$ ,  $\varphi_1(\zeta)$  and  $\psi_1(\zeta)$ ,  $\varphi_2(\zeta)$  and  $\psi_2(\zeta)$  are derived, with given values of ( $R_0, R_1, R_2, \sigma_v, \sigma_h, p_0, \mu_0, \mu_1, \mu_2, E_0, E_1, E_2, E_3, \eta, Ne, S, n, L, d$ ), the stresses and displacements in the linings and surrounding rock can be obtained.

#### 2.5.1. Stress and Displacement Components in the Linings

For primary lining:

$$\sigma_\rho^p + \sigma_\theta^p = 4 \operatorname{Re}[\varphi_1'(\zeta)/\omega'(\zeta)], \quad (2.36)$$

$$\sigma_\theta^p - \sigma_\rho^p \sigma_\theta + 2i\tau_{\rho\theta}^p = \frac{2\zeta^2}{\rho^2} \frac{1}{\omega'(\zeta)} \left\{ \frac{\varphi_1''(\zeta)\omega'(\zeta) - \varphi_1'(\zeta)\omega''(\zeta)}{[\omega'(\zeta)]^2} + \psi_1'(\zeta) \right\}. \quad (2.37)$$

For secondary lining:

$$\sigma_\rho^s + \sigma_\theta^s = 4 \operatorname{Re}[\varphi_2'(\zeta)/\omega'(\zeta)], \quad (2.38)$$

$$\sigma_\theta^s - \sigma_\rho^s \sigma_\theta + 2i\tau_{\rho\theta}^s = \frac{2\zeta^2}{\rho^2} \frac{1}{\omega'(\zeta)} \left\{ \frac{\varphi_2''(\zeta)\omega'(\zeta) - \varphi_2'(\zeta)\omega''(\zeta)}{[\omega'(\zeta)]^2} + \psi_2'(\zeta) \right\}. \quad (2.39)$$

where  $\sigma_\theta, \sigma_\rho, \tau_{\rho\theta}$  are the stress components in orthogonal curvilinear coordinates in the  $z$  plane. And the displacement for any point within the primary lining and secondary lining can be solved by substituting  $\varphi_1(\zeta)$  and  $\psi_1(\zeta)$ ,  $\varphi_2(\zeta)$  and  $\psi_2(\zeta)$  into Eq. (2.6) and (2.7), respectively.

#### 2.5.2. Stress and Displacement Components in the Surrounding Rock

The stress component at any point in the surrounding rock can be solved as follows:

$$\sigma_\rho^r + \sigma_\theta^r = 4 \operatorname{Re}[\varphi_5'(\zeta)/\omega'(\zeta)], \quad (2.40)$$

$$\sigma_\theta^r - \sigma_\rho^r + 2i\tau_{\rho\theta}^r = \frac{2\zeta^2}{\rho^2} \frac{1}{\omega'(\zeta)} \left\{ \frac{\varphi_5''(\zeta)\omega'(\zeta) - \varphi_5'(\zeta)\omega''(\zeta)}{[\omega'(\zeta)]^2} + \psi_5'(\zeta) \right\}, \quad (2.41)$$

where

$$\varphi_5(\zeta) = \Gamma\omega(\zeta) + \varphi_0(\zeta) + \varphi_3(\zeta) + \varphi_4(\zeta), \quad (2.42)$$

$$\psi_5(\zeta) = \Gamma'\omega(\zeta) + \psi_0(\zeta) + \psi_3(\zeta) + \psi_4(\zeta). \quad (2.43)$$

$\Gamma = (\sigma_v + \sigma_h)/4$  and  $\Gamma' = (\sigma_v - \sigma_h)/2$ . The first term of Eqs. (2.42) and (2.43) represent the corresponding analytic function before excavation, and the remaining terms reflect the effects of the primary lining, bolts, and the excavation on the surrounding rock mass, respectively.

### 3. EXAMPLE AND ANALYSIS

Use the following values for the relevant parameters: the radius of circular tunnel  $R_0 = 2.3$  m; the thickness of primary lining is 0.3 m ( $R_1 = 2.0$  m); the thickness of secondary lining is 0.4 m ( $R_2 = 1.6$  m); the vertical in-situ stress  $\sigma_v = 3$  MPa; the horizontal in-situ stress  $\sigma_h = 2$  MPa; the inner hydrostatic pressure  $p_0 = 0.1$  MPa; the Young's modulus of the rock mass, primary lining and secondary lining are  $E_0 = 5$  GPa,  $E_1 = 20$  GPa,  $E_2 = 10$  GPa, respectively; the Poisson's ratio of the rock mass and the double linings are  $\mu_1 = \mu_2 = \mu_3 = 0.25$ ; the coefficient of displacement released  $\eta = 0.0$ ; the terms of the series  $Ne = 8$ ; 12 bolts are installed into the tunnel, and each bolt is arranged every  $30^\circ$  from the horizontal; the length of bolts  $L = 1.5$  m; the diameter of bolts  $d = 2.5$  cm; the row spacing of bolts  $S = 1.0$  m; the Young's modulus of the bolts is  $E_3 = 210$  GPa. And Fig. 3 present the displacement solution and stress solution on the boundary of secondary lining and primary lining (both inner and outer). Due to symmetry, results from  $\theta = 0^\circ$  to  $\theta = 90^\circ$  are shown.

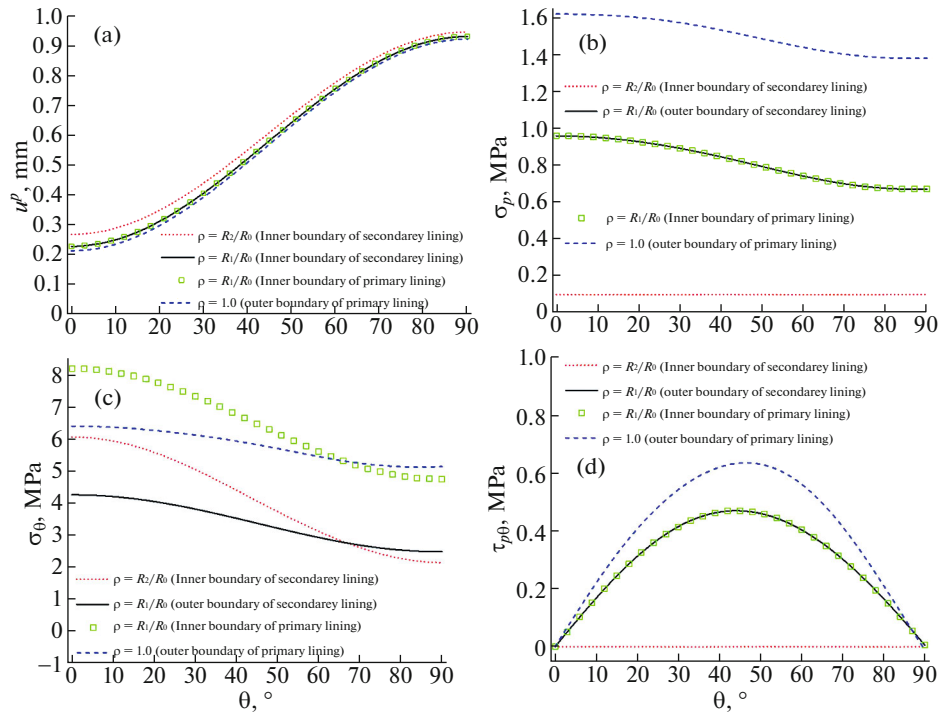


Fig. 3. Displacement and stress solution within the double linings.

It can be seen from the Fig. 3a, the closer to the center of the hydraulic tunnel, the greater the displacement of the lining boundary, and the displacement of the linings in the direction of the maximum in-situ stress ( $90^\circ$ ) is the largest, the displacement of the lining in the direction of the minimum in-situ stress ( $0^\circ$ ) is the smallest, which is consistent with the actual situation. From the Figs. 3a and 3d, it can be found that the radial stress and shear stress of the inner boundary of the secondary lining is 0.1 MPa and 0 MPa, respectively, which conforms to our preset boundary conditions. In addition, by comparing the results of radial displacements, radial stresses and shear stresses of contact interface of double linings in Figs. 3a, 3b and 3d, we can easily find that they are basically equal (green symbol and black line basically coincide), that is, they meet the displacement and stress continuity condition, that is so called “complete contact”.

Besides, the axial force of 12 point anchored rock bolts can be calculated by the method proposed in this paper. Similarly, due to symmetry, only the axial force of bolts installment in the direction of  $0^\circ$ ,  $30^\circ$ ,  $60^\circ$  and  $90^\circ$  are provided here, that is: 7.53 kN, 11.26 kN, 18.80 kN and 22.68 kN respectively. From these data, we know that the axial forces distribution of the bolts obtained are in line with the actual laws: the bolt with the maximum axial forces is in the direction of the maximum in-situ stress, and the bolt with the minimum axial force is in the direction of the minimum in-situ stress.

To a large extent, the effectiveness of this modeling is proved.

### 3.1. The Effect of Inner Hydrostatic Pressure

Use the same values for the relevant parameters, except for hydrostatic pressure on the inner boundary of the secondary lining. Let  $p_0 = 0.1$  MPa, 0.3 MPa, 0.5 MPa respectively. And then adopt the proposed approach, the axial forces of the bolts at different angles, radial displacement, and difference between maximum principal stress and minimum principal stress  $\sigma_1 - \sigma_3$  for the points at the boundary of the double linings can be plotted as follows.

It can be seen from the Fig. 4a, the axial forces of the bolts drop with the increase of the hydrostatic pressure, which is the same with the radial displacement for the points at the boundary of the double linings with different  $p_0$  in Fig. 4b. Similarly,  $\sigma_1 - \sigma_3$  of the points on different boundary decrease with the increase of inner hydrostatic pressure  $p_0$ . By the way, since the radial displacement of the interface between primary lining and primary lining is continuous, only the results of one boundary are showed in Fig. 4b.  $R_1$  and  $R'_1$  means at the outer boundary of the secondary lining and inner boundary of the primary lining,

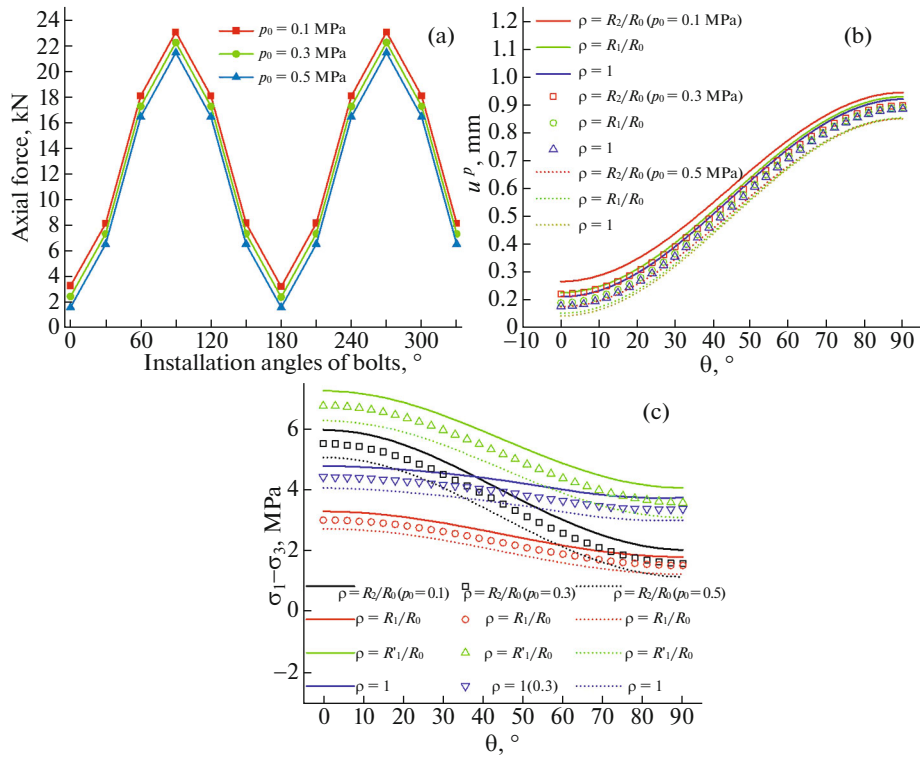


Fig. 4. Results with different inner hydrostatic pressures (a) axial force; (b) displacement (c)  $\sigma_1 - \sigma_3$ .

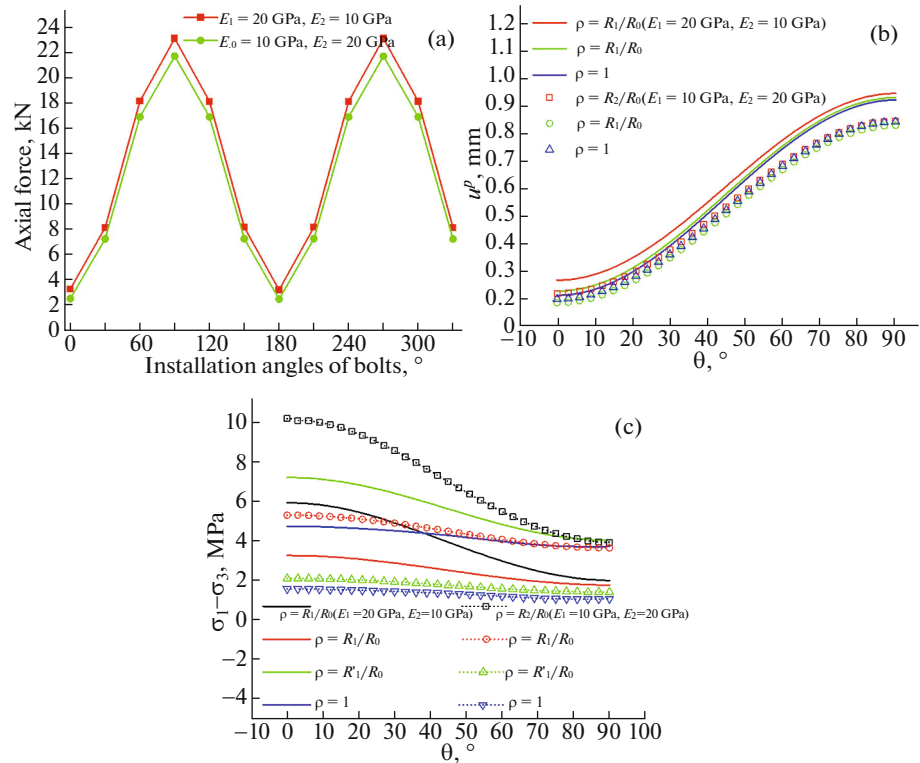


Fig. 5. Comparison of results before and after exchange of Young's modulus of double linings (a) axial force; (b) displacement (c)  $\sigma_1 - \sigma_3$ .

respectively. The fact is that the smaller the difference ( $\sigma_1 - \sigma_3$ ), the less prone to yield and failure. Therefore, the internal water pressure in a certain range can support the lining and surrounding rock.

### 3.2. The Effect Young's Modulus of the Linings

Similarly, use the same values for the relevant parameters, except for the Young's modulus of the double linings. Exchange the Young's modulus of primary lining and secondary lining, that is:  $E_1 = 10$  GPa,  $E_2 = 20$  GPa. And then adopt the proposed approach, compare the results after changing the Young's modulus with the results in example.

It can be seen from the Fig. 5a, after exchange of Young's modulus of double linings, the change of axial force of bolts is not obvious with only slightly reduce. The same law with the displacement results in Fig. 5b. But the displacements of points on the outer boundary of primary lining exceed that of interface of double linings. And as for  $\sigma_1 - \sigma_3$  of the points within secondary lining, no matter outer and inner boundary, it increases a lot. On the contrary,  $\sigma_1 - \sigma_3$  of the points within primary boundary decreases. That is to say, after exchange of Young's modulus of double linings, the support provided by the linings for the surrounding rock doesn't not change much. Only the stress distribution is adjusted in the two-layer lining itself. The one with large Young's modulus, that is, relatively hard, bears more loads.

## 4. CONCLUSIONS

A mechanical model for a deeply buried circular hydraulic tunnel supported by double linings and point anchored bolts is proposed by using the complex function method. The surrounding rock, primary lining and secondary lining, as well as bolts are linked together based on the complete contact condition. Through the contact surface continuity conditions and boundary conditions, the coefficients of the relevant analytical functions are solved, which attributes to the establishment of relevant linear equations. And then the axial forces of bolts, displacement and stress components of any point in the surrounding rock and double linings are derived.

Besides, the effect of inner hydrostatic pressure on the inner boundary of secondary lining and the influence of exchange of Young's modulus of double linings are discussed and achieve the following conclusions: (1) the internal water pressure can help support the lining and surrounding rock, decreasing the axial force of bolts, the displacement and  $\sigma_1 - \sigma_3$  of linings and surrounding rock. But it needs to be within a certain range, otherwise there will be a negative effect with generating tensile stress. (2) the exchange of Young's modulus of double linings, the support provided by the linings for the surrounding rock doesn't not change much. But the stress distribution will adjust itself within the two-layer lining. The one with larger Young's modulus, that is, relatively hard, bears more loads.

## REFERENCES

1. E. Leca and G.W. Clough, "Preliminary design for NATM tunnel support in soil," *J. Geotech. Eng.* **118** (4), 558–575 (1992).  
[https://doi.org/10.1016/0148-9062\(92\)92087-s](https://doi.org/10.1016/0148-9062(92)92087-s)
2. G. R. Dasari and M. D. Bolton, "Numerical modelling of a NATM tunnel construction in London Clay," in *Proc. of the Int. Symposium on Geotechnical Aspects of Underground Construction in Soft Ground* (Balkema, Rotterdam, 1996), pp. 491–496.
3. M. Karakus and R. J. Fowell, "FEM analysis for the effects of the NATM construction technique on settlement above shallow soft ground tunnels," *Educational Res.* **22** (5), 31–33 (2000).
4. C. Pichler, R. Lackner, L. Martak, et al., "Optimization of jet-grouted support in NATM tunnelling," *Int. J. Num. Anal. Met. Geomech.* **28** (7–8), 781–796 (2004).  
<https://doi.org/10.1002/nag.366>
5. M. M. de Farias, Á. H. Moraes Jr., and A. P. de Assis, "Displacement control in tunnels excavated by the NATM: 3-D numerical simulations," *Tunn. Underg. Sp. Tech.* **19** (3), 283–293 (2004).  
<https://doi.org/10.1016/j.tust.2003.11.006>
6. H. Schuller and H. F. Schweiger, "Application of a multilaminate model to simulation of shear band formation in NATM-tunnelling," *Comput. Geotech.* **29** (7), 501–524 (2002).  
[https://doi.org/10.1016/S0266-352X\(02\)00013-7](https://doi.org/10.1016/S0266-352X(02)00013-7)
7. P. G. C. Prazeres, K. Thoeni, and G. Beer, "Nonlinear analysis of NATM tunnel construction with the boundary element method," *Comput. Geotech.* **40**, 160–173 (2012).  
<https://doi.org/10.1016/j.compgeo.2011.10.005>

8. M. Y. Ren, Q. Y. Zhang, Z. J. Zhang, et al., "Study on mechanism of segmental lining-bolt combined support for deep-buried tunnel," *Geotech. Geol. Eng.* **37** (5) (2019).  
<https://doi.org/10.1007/s10706-019-00860-x>
9. N. S. Bulychev, *Underground Construction Mechanics* (Nedra, Moscow, 1982).
10. C. Atkinson and D. A. Eftaxiopoulos, "A plane model for the stress field around an inclined, cased and cemented wellbore," *Int. J. Numer. Anal. Meth. Geomech.* **20** (8), 549–569 (1996).  
[https://doi.org/10.1002/\(SICI\)1096-9853\(199608\)20:8<549::AID-NAG838>3.0.CO;2-U](https://doi.org/10.1002/(SICI)1096-9853(199608)20:8<549::AID-NAG838>3.0.CO;2-U)
11. M. B. Wang and S. C. Li, "A complex variable solution for stress and displacement field around a lined circular tunnel at great depth," *Int. J. Numer. Anal. Meth. Geomech.* **33** (7), 939–951 (2009).  
<https://doi.org/10.1002/nag.749>
12. A. Z. Lu, L. Q. Zhang, and N. Zhang, "Analytic stress solutions for a circular pressure tunnel at pressure and great depth including support delay," *Int. J. Rock. Mech. Min. Sci.* **48** (3), 514–519 (2011).  
<https://doi.org/10.1016/j.ijrmms.2010.09.002>
13. A. Z. Lu, N. Zhang, and L. Kuang, "Analytic solutions of stress and displacement for a non-circular tunnel at great depth including support delay," *Int. J. Rock. Mech. Min. Sci.* **70**, 69–81 (2014).  
<https://doi.org/10.1016/j.ijrmms.2014.04.008>
14. A. Z. Lu, N. Zhang, and Y. Qin, "Analytical solutions for the stress of a lined non-circular tunnel under full-slip contact conditions," *Int. J. Rock. Mech. Min. Sci.* **79**, 183–192 (2015).  
<https://doi.org/10.1016/j.ijrmms.2015.08.008>
15. A. Z. Lu, and L. Q. Zhang, *Complex Function Method on Mechanical Analysis of Underground Tunnel* (Science Press, Beijing, 2007).
16. N. I. Muskhelishvili, *Some Basic Problems of The Mathematical Theory of Elasticity* (Groningen, Noordhoff, 1963).
17. E. Hoek and E. T. Brown, *Underground Excavations in Rock* (The Institution of Mining and Metallurgy, London, 1982).
18. C. Li and B. Stillborg, "Analytical models for rock bolts," *Int. J. Rock. Mech. Min. Sci. Abstr.* **36**, 1013–1029 (1999).  
[https://doi.org/10.1016/S1365-1609\(99\)00064-7](https://doi.org/10.1016/S1365-1609(99)00064-7)
19. S. H. Chen, S. Qiang, S. F. Chen, et al., "Composite element model of the fully grouted rock bolt". *Rock. Mech. Rock. Eng.* **37** (3), 193–212 (2004).  
<https://doi.org/10.1007/s00603-003-0006-z>
20. Y. Cai, T. Esaki, and Y. Jiang, "A rock bolt and rock mass interaction model," *Int. J. Rock. Mech. Min. Sci.* **41**, 1055–1067 (2004).  
<https://doi.org/10.1016/j.ijrmms.2004.04.005>
21. Y. Cai, T. Esaki, and Y. Jiang, "An analytical model to predict axial load in grouted rock bolt for soft rock tunneling," *Tunn. Under. Sp. Tech.* **19** (6), 607–618 (2004).  
<https://doi.org/10.1016/j.tust.2004.02.129>
22. A. Z. Lu, Y. J. Liu, and X. L. Zhang, "A theoretical solution for a circular tunnel reinforced by fully grouted rock bolt," *Chinese J. Rock Mech. Eng.* **37** (7), 1561–1573 (2018).  
<https://doi.org/10.13722/j.cnki.jrme.2018.0163>
23. A. Z. Lu and E. H. Zhu, "An analytical method for determining the axial force of point anchored rockbolts in an elliptical tunnel," *Chinese J. Rock Mech. Eng.* **38**, 1–12 (2019).  
<https://doi.org/10.13722/j.cnki.jrme.2018.1473>
24. I. W. Farmer, "Stress distribution along resin grouted rock anchor," *Int. J. Rock Mech. Min. Sci.* **12**, 347–351 (1975).  
[https://doi.org/10.1016/0148-9062\(75\)90168-0](https://doi.org/10.1016/0148-9062(75)90168-0)
25. T. J. Freeman, "The behaviour of fully-bonded rock bolts in the Kielder experimental tunnel," *Tunn. Tunnlg.* **10** (5), 37–40 (1978).  
[https://doi.org/10.1016/0148-9062\(78\)91073-2](https://doi.org/10.1016/0148-9062(78)91073-2)
26. S. Bjurstrom, "Shear strength of hard rock joints reinforced by grouted untensioned bolts," in *Advances in Rock Mechanics: Proceedings of the 3rd Congress of the International Society for Rock Mechanics* (National Academy of Sciences, Washington, D.C., 1974), Vol. II B, pp. 1194–1999.
27. B. Benmokrane, A. Chennouf, and H. S. Mitri, "Laboratory evaluation of cementbased grouts and grouted rock anchors." *Int. J. Rock Mech. Min. Sci. Geomech. Abstr.* **32**, 633–642 (1995).  
[https://doi.org/10.1016/0148-9062\(95\)00021-8](https://doi.org/10.1016/0148-9062(95)00021-8)
28. D. Bernaud, P. D. Buhan, and S. Maghous, "Numerical simulation of the convergence of a bolt-supported tunnel through a homogenization method," *Int. J. Numer. Anal. Methods Geomech.* **19**, 267–288 (1995).  
<https://doi.org/10.1002/nag.1610190404>
29. A. Bobet, "A simple method for analysis of point anchored rockbolts in circular tunnels in elastic ground," *Rock Mech. Rock Eng.* **39** (4), 315–338 (2006).  
<https://doi.org/10.1007/s00603-005-0066-3>

30. S. H. Chen, C. H. Fu, S. Isam, "Finite element analysis of jointed rock masses reinforced by fully-grouted bolts and shotcrete lining," *Int. J. Rock Mech. Min.* **46** (1), 19–30 (2009).  
<https://doi.org/10.1016/j.ijrmms.2008.03.002>
31. J. Holmgren and A. Ansell, "Design of Bolt Anchored Reinforced Shotcrete Linings Subjected to Impact Loadings," in *Shotcrete for Underground Support X*, Ed. by D. R. Morgan and H. W. Parker (ASCE, Reston, Virginia, 2006), pp. 72-88.  
[https://doi.org/10.1061/40885\(215\)7](https://doi.org/10.1061/40885(215)7)
32. Y. Sun and D. L. Zhang, "Synergy principle of complex supporting structural systems in tunnels," *Eng. Mech.* **33**, 52–62 (2016).  
<https://doi.org/10.6052/j.issn.1000-4750.2016.05.ST04>
33. M. Y. Ren, Q. Y. Zhang, Z. J. Zhang, et al., "Study on mechanism of segmental lining-bolt combined support for deep-buried tunnel," *Geotech. Geol. Eng.* **37** (5), (2019).  
<https://doi.org/10.1007/s10706-019-00860-x>
34. Z. T. Bieniawski, *Engineering Rock Mass Classification* (John Wiley and Sons, New York, 1989).
35. N. R. Barton, R. Lien, and J. Lunde, "Engineering classification of rock masses for the design of rock support," *Rock Mech.* **6**(4), 189–236 (1974).  
<https://doi.org/10.1007/BF01239496>